

Lifetime of edge modes at rough surfaces of chiral superconductors

Seiji Higashitani, Gota Sato, and Yasushi Nagato

Graduate School of Advanced Science and Engineering, Hiroshima University,
1-7-1 Kagamiyama, Higashi-Hiroshima City, Hiroshima, 739-8521, Japan

(Dated: August 13, 2024)

We study the effect of diffuse surface scattering on the edge modes in two-dimensional chiral superconductors with time-reversal symmetry-breaking Cooper pairs, each carrying angular momentum $m\hbar$ ($m = 1, 2, 3, \dots$). To elucidate the diffuse scattering effect, we formulate the inverse lifetime $\Gamma = \hbar/\tau$ corresponding to the broadening of the surface density of states (SDOS) for the edge mode. This derivation uses random S-matrix theory, which allows us to describe the surface effect in a unified way from the specular to the diffuse limit within the quasiclassical theory framework of superconductivity. We find that Γ in the chiral states with $m \geq 2$ is larger than that in the chiral p -wave state ($m = 1$) because of the multiple edge mode branches in former superconducting states (the number of which equals m). Diffuse scattering between the different branches causes a significant broadening of SDOS. In contrast, the edge mode in the chiral p -wave state is robust to diffuse scattering because only a single edge mode branch exists. We also discuss SDOS at the diffuse limit, where the description in terms of Γ is not useful. The diffuse scattering effect on SDOS can be understood qualitatively in terms of destructive interference analogous to that caused by impurity scattering in unconventional superconductors.

I. INTRODUCTION

Since the discovery of superfluid ^3He , Cooper pair condensates with time-reversal symmetry-breaking chiral order have been of continuing interest in condensed matter physics. It is well established that spin-triplet p -wave pairing is realized in superfluid ^3He and the superfluid ^3He -A phase is in the chiral p -wave pairing state [1]. Triplet pairing analogous to superfluid ^3He was proposed for the quasi-two-dimensional (2D) superconductivity in Sr_2RuO_4 shortly after its discovery [2, 3]. Subsequent experiments supported the 2D chiral p -wave state among the proposed candidates [4]. This has led to numerous theoretical investigations into 2D chiral p -wave superconductivity (note, the pairing symmetry of Sr_2RuO_4 has recently been reexamined and is currently under discussion [5]). The 2D chiral p -wave state belongs to the group of pairing states characterized by the gap function $\propto (\hat{k}_x \pm i\hat{k}_y)^m$, where $\hat{k} = (\hat{k}_x, \hat{k}_y)$ is the unit vector along the Fermi wavevector and $m = 1, 2, 3, \dots$. The case of $m = 1$ corresponds to the chiral p -wave state.

The surface state of unconventional (non- s -wave) superconductors differs from that of the bulk state. The surface physics in the chiral superfluid and superconductors are highlighted by the gapless edge mode, which induces an edge current along the surface [6–22]. In the chiral p -wave state, the edge current carried by the edge mode is sizable at low temperatures. According to the quasiclassical theory of superconductivity, the corresponding mass current at absolute zero is estimated to be $n\hbar/2$ with n being the number density of fermions [7–10]. However, the edge mass current vanishes in higher-order chiral states, such as those with d -wave ($m = 2$) and f -wave ($m = 3$) orbital symmetry [11–14]. This contrasting result is because, unlike the p -wave state, the higher-order states have multiple edge-mode branches and their contributions to the mass current cancel out. Moreover,

the orbital symmetry-dependent feature of chiral superconductivity manifests in the edge current density at a rough surface. In real systems, surfaces inevitably have microscopic irregularities that are sufficient for quasiparticles to diffusely scatter and suppress the edge current density. Diffuse scattering effects on the chiral superconductivity have been extensively studied as an important factor affecting the observability of edge currents [16–22]. According to the numerical analysis of Suzuki and Asano [20], the influence of diffuse scattering is weak for the chiral p - and d -wave states but is substantial for the chiral f -wave state that the edge current density is almost suppressed to zero.

In this work, we focus on the broadening of the surface density of states (SDOS) for the edge mode caused by diffuse scattering. In particular, we ask the following questions that have not been addressed in detail: what is the main scattering process that broaden SDOS of the edge mode and to what extent does the magnitude of the broadening differ among chiral superconductors with different orbital symmetry? To address these questions, we formulate SDOS in terms of a surface self-energy that contains information about the lifetime of the edge mode. We use the random S-matrix theory, which provides a closed set of quasiclassical equations to describe the rough surface effect on superconductivity [23–26].

The remaining paper is organized as follows. In Section II, we describe our theoretical model. In Section III, we briefly review the edge mode formed at a specular surface of the 2D chiral superconductors and classify the edge mode into two. This classification is important for understanding the effects of diffuse scattering on the edge modes. In Section IV, the general formula for SDOS is derived based on the random S-matrix theory and some numerical results of SDOS are presented. In Section V, we first introduce the surface self-energy for

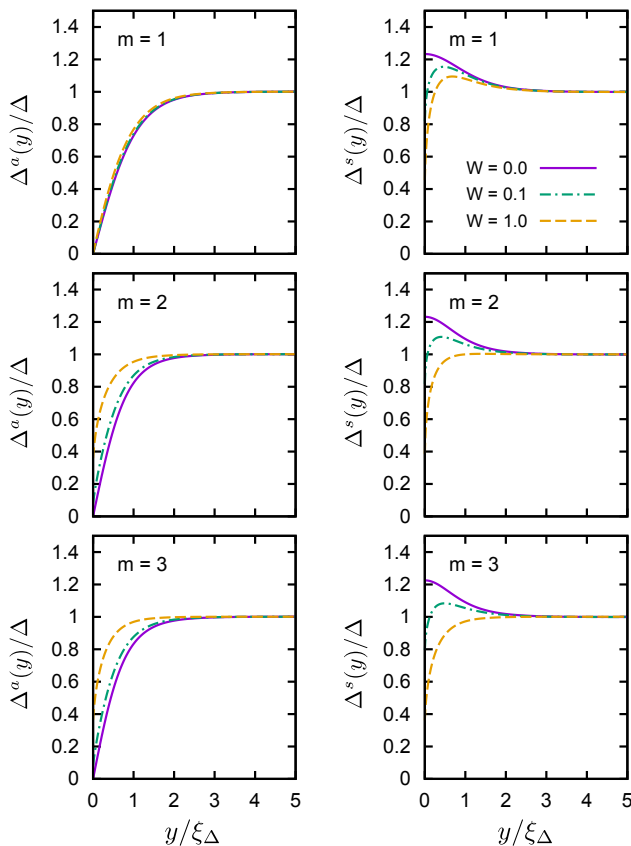


FIG. 1. Spatial dependence of $\Delta^a(y)$ (left panels) and $\Delta^s(y)$ (right panels) for $m = 1, 2, 3$ at $W = 0.0, 0.1, 1.0$. The results are calculated at $T = 0.2T_c$, where T_c is the transition temperature. The distance y from the surface is scaled by the coherence length $\xi_\Delta = \hbar v_F / \Delta$.

the edge mode, and then derive an approximate formula for subgap SDOS, which applies to the case where the diffuse scattering probability is sufficiently small and the edge mode is well defined. The approximate formula is used to define the inverse lifetime $\Gamma = \hbar/\tau$ of the edge mode. Additionally, we briefly discuss SDOS in the diffuse limit, where the scattering is completely diffuse. The final section presents the conclusion.

II. MODEL

We consider a semi-infinite 2D superconductor occupying the $y > 0$ space and with a rough surface along the x -axis. The surface is assumed to be macroscopically flat but with atomic-scale irregularity. The superconducting state is characterized by the following chiral gap function in the bulk:

$$\Delta(y \rightarrow \infty, \hat{k}) = \Delta e^{im\phi}, \quad (1)$$

where Δ is the gap amplitude with a positive real value and $\hat{k} = (\hat{k}_x, \hat{k}_y) = (\cos \phi, \sin \phi)$. The orbital symmetry

of the gap function is classified by an integer m . For example, $m = 1, 2, 3$ corresponds to the p -, d -, and f -wave superconductors, respectively. The bulk gap function, defined as a spin space matrix, has the form $\Delta e^{im\phi} i\sigma_2$ for the singlet superconductors with even m and $\Delta e^{im\phi} \sigma_1$ for the triplet superconductors with odd m , where σ_i ($i = 1, 2, 3$) are Pauli matrices.

Surface scattering is known to cause a spatial variation of the gap function. Consequently, the gap function takes the following form:

$$\Delta(y, \hat{k}) = \Delta^s(y, \phi) + i\Delta^a(y, \phi), \quad (2)$$

where Δ^s and Δ^a denote the symmetric and antisymmetric components with respect to the transformation $\phi \rightarrow -\phi$, respectively, i.e.,

$$\Delta^s(y, \phi) = \Delta^s(y) \cos(m\phi), \quad (3)$$

$$\Delta^a(y, \phi) = \Delta^a(y) \sin(m\phi). \quad (4)$$

$\Delta^s(y)$ and $\Delta^a(y)$ asymptotically approach the bulk value Δ as $y \rightarrow \infty$. Typical examples of the self-consistently determined spatial dependence of $\Delta^s(y)$ and $\Delta^a(y)$ are shown in Fig. 1, where the parameter W controls the diffuse scattering probability [see Eq. (18) and below for details]. Similar results for the rough surface effect on the self-consistent gap functions in the chiral p -, d -, and f -states can be found in Refs. 13 and 20.

When analyzing the boundary problem in the semi-infinite superconductor, it is convenient to restrict the domain of ϕ to $[0, \pi]$ and specify the position on the Fermi surface by the unit vector $\hat{k}_\alpha = (\cos \phi, \alpha \sin \phi)$ with $\sin \phi > 0$ and $\alpha = \pm$. Accordingly, Eq. (2) is expressed as

$$\Delta(y, \hat{k}_\alpha) = \Delta^s(y, \phi) + \alpha i \Delta^a(y, \phi) \equiv \Delta_\alpha(y, \phi). \quad (5)$$

The gap function $\Delta_\pm(y, \phi)$ corresponds to the pair potential felt by a quasiparticle on the Fermi surface with a wave function $\propto e^{ik_\parallel x \pm ik_\perp y}$, where $k_\parallel = k_F \cos \phi$ and $k_\perp = k_F \sin \phi$.

III. EDGE MODE AT SPECULAR SURFACE

When the surface is specular, the quasiparticle states in the above model system can be described by the wave function

$$\psi(x, y) = e^{ik_\parallel x} [\varphi_+(y)e^{ik_\perp y} + \varphi_-(y)e^{-ik_\perp y}]. \quad (6)$$

Within quasiclassical approximation, which is legitimate for weak-coupling superconductors with Δ sufficiently smaller than the Fermi energy, $\varphi_\alpha(y)$ obeys the Andreev equation

$$\begin{pmatrix} -\alpha i \hbar v_\perp \partial_y & \Delta_\alpha(y, \phi) \\ \Delta_\alpha^*(y, \phi) & \alpha i \hbar v_\perp \partial_y \end{pmatrix} \varphi_\alpha(y) = E \varphi_\alpha(y), \quad (7)$$

where $v_{\perp} = v_F \sin \phi$ is the y -component of the Fermi velocity. Equation (7) has a solution that decays exponentially as y increases, corresponding to the edge mode. To obtain the energy and wave function of the edge mode, we adopt a uniform gap model, where $\Delta_{\alpha}(y, \phi)$ is replaced in all space by the bulk gap function $\Delta e^{\alpha i m \phi}$. Then, the edge mode, which satisfies the specular boundary condition $\psi(x, 0) = 0$, has the energy [11–14]

$$E_{\text{edge}} = -s_{\phi} \Delta \cos(m\phi), \quad s_{\phi} = \text{sgn}[\sin(m\phi)]. \quad (8)$$

The normalized wave function is

$$\psi_{\text{edge}}(x, y) = e^{ik_{\parallel}x} (e^{ik_{\perp}y} - e^{-ik_{\perp}y}) \varphi(y), \quad (9)$$

where

$$\varphi(y) = \sqrt{\kappa_0} e^{-\kappa_0 y} \left(\frac{1+s_{\phi}}{2} |1\rangle + \frac{1-s_{\phi}}{2} |2\rangle \right), \quad (10)$$

$$|1\rangle = \frac{1}{\sqrt{2}} \begin{pmatrix} 1 \\ -1 \end{pmatrix}, \quad |2\rangle = \frac{1}{\sqrt{2}} \begin{pmatrix} 1 \\ 1 \end{pmatrix}, \quad (11)$$

and $\kappa_0 = \Delta |\sin(m\phi)| / \hbar v_{\perp}$.

The edge mode consists of m branches, which are divided into two groups: $s_{\phi} = +1$ and $s_{\phi} = -1$. In Fig. 2, we plot the ϕ dependence of E_{edge} and number the branches ①, ②, ③, \dots in order of increasing ϕ . The odd- and even-numbered branches are in the $s_{\phi} = +1$ and $s_{\phi} = -1$ group, respectively. We refer to the edge states in the $s_{\phi} = +1$ group as O-mode and those in the $s_{\phi} = -1$ group as E-mode. As shown in Section V, the O- and E-modes are coupled via diffuse scattering when the surface is rough.

IV. METHOD

We apply the quasiclassical theory of superconductivity to the above model system. The theory can be formulated in terms of the quasiclassical Green's function $\hat{g}_{\alpha}(y)$, which is defined as a 2×2 matrix in particle-hole space and obeys the Eilenberger equation [27]

$$\alpha i \hbar v_{\perp} \partial_y \hat{g}_{\alpha}(y) = [\hat{g}_{\alpha}(y), \hat{h}_{\alpha}(y, \phi, \varepsilon)], \quad (12)$$

$$\hat{h}_{\alpha}(y, \phi, \varepsilon) = \begin{pmatrix} \varepsilon & \Delta_{\alpha}(y, \phi) \\ -\Delta_{\alpha}^*(y, \phi) & -\varepsilon \end{pmatrix}, \quad (13)$$

where ε is a complex energy variable. Equation (12) is supplemented by the normalization condition $\hat{g}_{\alpha}^2(y) = -1$. The normalized quasiclassical Green's function in the bulk is given as

$$\hat{g}_{\alpha}(\infty) = \frac{1}{\Omega} \hat{h}_{\alpha}(\infty, \phi, \varepsilon), \quad (14)$$

where $\Omega = \sqrt{\Delta^2 - \varepsilon^2}$.

In this work, we are interested in the angle-resolved SDOS

$$n(\phi, E) = \text{Im} \left[\frac{1}{2} \text{Tr} \sum_{\alpha=\pm} \frac{\hat{\rho}_3 \hat{g}_{\alpha}^R(0)}{2} \right], \quad (15)$$

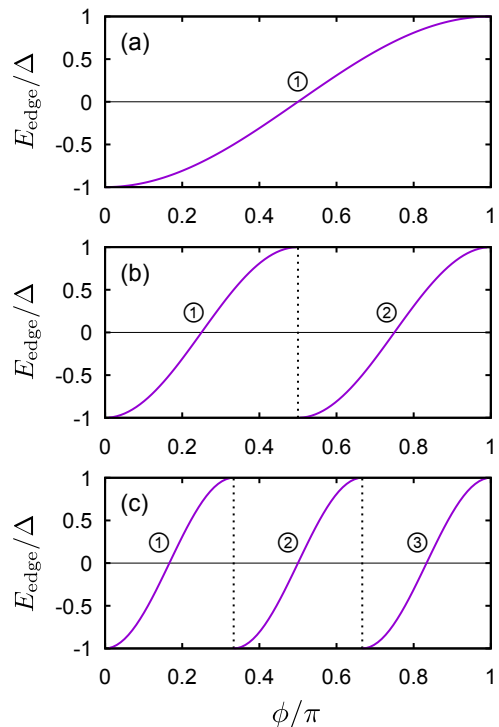


FIG. 2. Energy of the edge mode as a function of ϕ/π in the specular limit for 2D chiral superconductors with (a) p -wave ($m = 1$), (b) d -wave ($m = 2$), and (c) f -wave ($m = 3$) orbital symmetries.

where $\hat{\rho}_3$ is the third Pauli matrix in the particle-hole space and $\hat{g}_{\alpha}^R(y)$ is the retarded quasiclassical Green's function at $\varepsilon = E + i0^+$. The gap function $\Delta_{\alpha}(y, \phi)$ in Eq. (13) is determined using the off-diagonal elements of the quasiclassical Matsubara Green's function at $\varepsilon = i(2n + 1)\pi k_B T$, where $n = 0, \pm 1, \pm 2, \dots$ (for details, see Ref. 14).

The quasiclassical Green's function is required to asymptotically reach $\hat{g}_{\alpha}(\infty)$ as $y \rightarrow \infty$ and to satisfy a surface boundary condition at $y = 0$. When the surface is specular, $\hat{g}_{\alpha}(0)$ satisfies

$$\hat{g}_{+}(0) = \hat{g}_{-}(0) \equiv \hat{g}_S. \quad (16)$$

This boundary condition implies that the quasiclassical propagator on the specular reflection trajectory is continuous at the surface. When the surface is rough, this property is lost due to diffuse scattering. According to the random S-matrix theory, the boundary condition is modified as [23–26]

$$\hat{g}_{+}(0) = \frac{1 + i\hat{\gamma}}{1 - i\hat{\gamma}} \hat{g}_{-}(0) \frac{1 - i\hat{\gamma}}{1 + i\hat{\gamma}}. \quad (17)$$

The matrix $\hat{\gamma}$ carries information on diffuse scattering

effects and is self-consistently determined using

$$\hat{\gamma} = 2W \left\langle \frac{1}{\hat{g}_S^{-1} - \hat{\gamma}} \right\rangle_\phi, \quad (18)$$

$$\langle \cdots \rangle_\phi = \frac{\sum_{k_\parallel} (\cdots)}{\sum_{k_\parallel} 1} = \frac{1}{2} \int_0^\pi d\phi \sin \phi (\cdots), \quad (19)$$

where the parameter W takes a value from zero to unity. The case $W = 0$ corresponds to the specular limit and $W = 1$ to the diffuse limit at which an incident quasiparticle is scattered isotropically. The rough surface effect can be parameterized by specularity R , defined as the specular reflection probability for an electron at the Fermi level in the normal state. The relationship between W and R is given by $W = (1 - \sqrt{R})/(1 + \sqrt{R})^2$ [26]. In the intermediate regime between $W = 0$ ($R = 1$) and $W = 1$ ($R = 0$), specular reflection and diffuse scattering occur with probability R and $1 - R$, respectively.

The quasiclassical Green's function that satisfies the normalization and boundary conditions can be expressed as (see Appendix A)

$$\hat{g}_+(y) = \frac{2i\hat{\rho}_3}{1 - D(y)F(y)} \begin{pmatrix} 1 \\ D(y) \end{pmatrix} (1 - F(y)) - i, \quad (20)$$

$$\hat{g}_-(y) = \frac{2i\hat{\rho}_3}{1 - D(y)F(y)} \begin{pmatrix} 1 \\ F(y) \end{pmatrix} (1 - D(y)) - i, \quad (21)$$

where $D(y)$ and $F(y)$ obey the Riccati-type differential equations

$$i\hbar v_\perp \partial_y D = 2\varepsilon D - \Delta_+^*(y, \phi) - \Delta_+(y, \phi) D^2, \quad (22)$$

$$i\hbar v_\perp \partial_y F = -2\varepsilon F + \Delta_-^*(y, \phi) + \Delta_-(y, \phi) F^2, \quad (23)$$

along with the boundary conditions

$$D(\infty) = \frac{\Delta e^{-im\phi}}{\varepsilon + i\Omega}, \quad (24)$$

$$\begin{pmatrix} 1 \\ F(0) \end{pmatrix} \propto \hat{\rho}_3 \frac{1 - i\hat{\gamma}}{1 + i\hat{\gamma}} \hat{\rho}_3 \begin{pmatrix} 1 \\ D(0) \end{pmatrix}. \quad (25)$$

We note that $F(0) = D(0)$ holds in the specular limit and the following expression for \hat{g}_S is obtained.

$$\hat{g}_S = \hat{\rho}_3 (G_1 |1\rangle\langle 1| + G_2 |2\rangle\langle 2|), \quad (26)$$

where

$$G_1 = i \frac{1 - D(0)}{1 + D(0)}, \quad G_2 = i \frac{1 + D(0)}{1 - D(0)}. \quad (27)$$

In the next section, we show that G_1 and G_2 have the O- and E-mode poles, respectively. The $\hat{\gamma}$ matrix can be parameterized in a form similar to Eq. (26), i.e.,

$$\hat{\gamma} = \hat{\rho}_3 (S_1 |1\rangle\langle 1| + S_2 |2\rangle\langle 2|). \quad (28)$$

Substituting Eq. (28) into Eq. (18), we determine $S_{1,2}$ as

$$S_1 = 2W \left\langle \frac{1}{G_1^{-1} - S_2} \right\rangle_\phi, \quad (29)$$

$$S_2 = 2W \left\langle \frac{1}{G_2^{-1} - S_1} \right\rangle_\phi. \quad (30)$$

For an arbitrary W , $F(0)$ is given as

$$F(0) = \frac{\mathbb{S}_1 \mathbb{S}_2 D(0) + (\mathbb{S}_1 - \mathbb{S}_2)/2}{1 - (\mathbb{S}_1 - \mathbb{S}_2)D(0)/2}, \quad (31)$$

where

$$\mathbb{S}_j = \frac{1 + iS_j}{1 - iS_j} \quad (j = 1, 2). \quad (32)$$

Equations (31), (20), and (21) leads to the following expression for SDOS.

$$n(\phi, E) = n_1(\phi, E) + n_2(\phi, E), \quad (33)$$

$$n_j(\phi, E) = \frac{1}{2} \text{Im}(\mathcal{G}_j^R) \quad (j = 1, 2), \quad (34)$$

where

$$\mathcal{G}_1 = i \frac{1 - \mathbb{S}_2 D(0)}{1 + \mathbb{S}_2 D(0)} = \frac{G_1 + S_2}{1 - S_2 G_1}, \quad (35)$$

$$\mathcal{G}_2 = i \frac{1 + \mathbb{S}_1 D(0)}{1 - \mathbb{S}_1 D(0)} = \frac{G_2 + S_1}{1 - S_1 G_2}. \quad (36)$$

The Green's functions \mathcal{G}_1 and \mathcal{G}_2 have the O- and E-mode poles affected by diffuse scattering, respectively.

The energy dependence of angle-resolved SDOS for $m = 1, 2, 3, 4$ and $W = 0.1$ ($R = 0.5$) obtained from Eqs. (33)-(36) within the uniform gap approximation is shown in the upper panels of Fig. 3. The angle is chosen to be $\phi = \pi/2m$ as an example. The results illustrate the robustness of the edge mode to diffuse scattering in the chiral p -wave superconductor ($m = 1$). For the p -wave, SDOS of the edge mode is sharply peaked even for the non-specular case ($W \neq 0$). In contrast, the broadening of SDOS peak is significant for higher-order chiral states ($m \geq 2$). In the next section, we clarify the reason for the robustness of the edge mode in the p -wave state.

V. SDOS OF THE EDGE MODE

To elucidate the diffuse scattering effect on the edge mode, we analyze SDOS under the uniform gap model, which allows analytical calculations. The influence of the spatially varying self-consistent gap function is discussed separately in Appendix B.

A. Subgap SDOS

Within the uniform gap model, $D(y)$ is a constant in space; thus, $D(0) = D(\infty)$. Then, $G_{1,2}$ can be written as

$$G_1 = -\frac{\Omega_1}{\varepsilon - E_1^0}, \quad G_2 = -\frac{\Omega_2}{\varepsilon - E_2^0}, \quad (37)$$

where

$$\Omega_1 = \Omega + \Delta \sin(m\phi), \quad \Omega_2 = \Omega - \Delta \sin(m\phi), \quad (38)$$

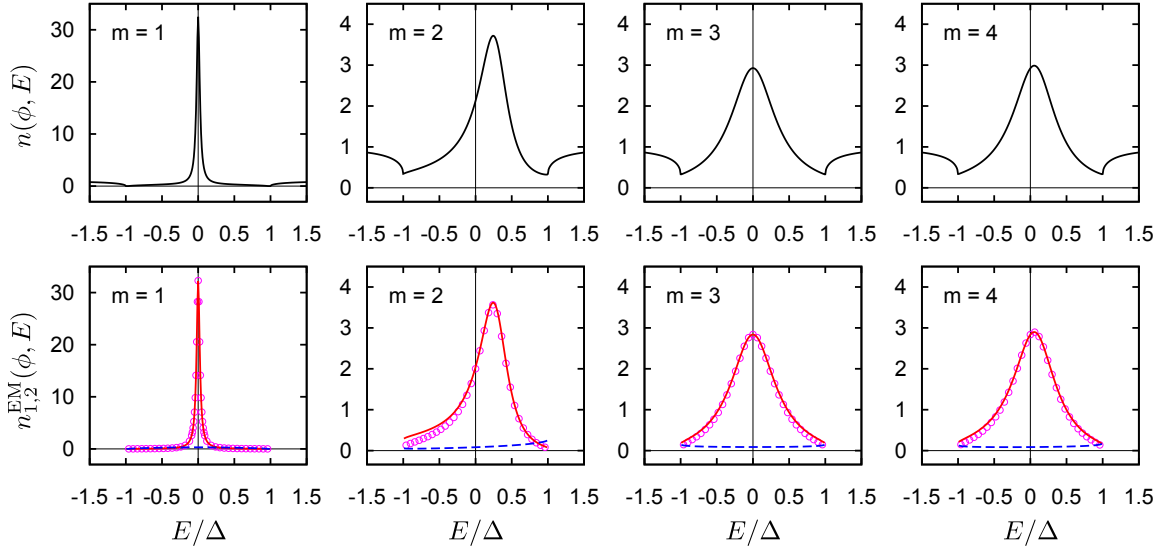


FIG. 3. Angle-resolved SDOS at a rough surface with $W = 0.1$ ($R = 0.5$) for $m = 1, 2, 3, 4$. The chosen angle is $\phi = \pi/2m$, where a zero mode ($E_{\text{edge}} = 0$) belonging to an O-mode branch appears in the specular limit. The upper panels show the results of $n(\phi, E) = n_1(\phi, E) + n_2(\phi, E)$. The lower panels are plots from Eq. (43) for the subgap SDOS $n_1^{\text{EM}}(\phi, E)$ (solid red lines) and $n_2^{\text{EM}}(\phi, E)$ (dashed blue lines). The open red circles correspond to the approximate formula (49) for the O-mode.

and $E_1^0 = -\Delta \cos(m\phi)$ and $E_2^0 = \Delta \cos(m\phi)$ are the energies of the O- and E-modes at the specular surface, respectively. From Eq. (37), we obtain the SDOS of the edge modes at the specular surface ($W = 0$) as

$$n_1^{\text{EM}}(\phi, E) = \frac{1 + s_\phi}{2} \pi \Delta |\sin(m\phi)| \delta(E - E_1^0), \quad (39)$$

$$n_2^{\text{EM}}(\phi, E) = \frac{1 - s_\phi}{2} \pi \Delta |\sin(m\phi)| \delta(E - E_2^0). \quad (40)$$

Equations (39) and (40) correspond to SDOS of the O- and E-modes, respectively.

To generalize these results to an arbitrary W , we substitute Eq. (37) into Eqs. (35) and (36). Then, we obtain

$$\mathcal{G}_1 = -\frac{\Omega_1 - (\varepsilon - E_1^0)S_2}{\varepsilon - E_1^0 + \Omega_1 S_2}, \quad (41)$$

$$\mathcal{G}_2 = -\frac{\Omega_2 - (\varepsilon - E_2^0)S_1}{\varepsilon - E_2^0 + \Omega_2 S_1}. \quad (42)$$

Taking the imaginary part of $\mathcal{G}_{1,2}^R$ for $|E| < \Delta$, we get

$$n_{j=1,2}^{\text{EM}}(\phi, E) = -\frac{\Sigma_j''}{2\Omega_j} \frac{\Omega_j^2 + (E - E_j^0)^2}{(E - E_j^0 - \Sigma_j')^2 + \Sigma_j''^2}. \quad (43)$$

Here, we introduce a surface self-energy defined as

$$\Sigma_{1,2} = -\Omega_{1,2} S_{2,1} \quad (44)$$

and denote the real and imaginary parts of the retarded self-energy as $\Sigma_{1,2}'$ and $\Sigma_{1,2}''$, respectively. Note that $\Sigma_{1,2}$ is proportional to $S_{2,1}$ (not $S_{1,2}$). This implies that diffuse scattering between O- and E-modes is critical in the rough surface effect on SDOS (see the next subsection).

B. Lifetime of the edge mode

When the surface is specular, the edge modes with energies $E_{1,2}^0$ have an infinite lifetime. Hence, their SDOS are expressed as delta-functions. In contrast, at rough surfaces, SDOS is broadened due to diffuse scattering. In this subsection, we discuss SDOS in the case $W \ll 1$, where the broadening is not large enough to obscure the well-defined edge modes.

Let the energies of the O- and E-modes at $W \neq 0$ be E_1 and E_2 , respectively. These energies can be defined as a solution of

$$E - E_j^0 - \Sigma_j' = 0 \quad (j = 1, 2). \quad (45)$$

We expand the left-hand side around $E = E_j$ and introduce a renormalization factor

$$Z_j = \frac{1}{1 - (\partial \Sigma_j' / \partial E)_{E=E_j}}. \quad (46)$$

Then, we obtain

$$E - E_j^0 - \Sigma_j' = (E - E_j) / Z_j. \quad (47)$$

Substituting Eq. (47) into Eq. (43) yields

$$n_j^{\text{EM}}(\phi, E) = -\frac{Z_j^2 \Sigma_j''}{2\Omega_j} \frac{\Omega_j^2 + (E - E_j^0)^2}{(E - E_j)^2 + (Z_j \Sigma_j'')^2}. \quad (48)$$

In the numerator, $(E - E_j^0)^2 \sim (E_j - E_j^0)^2$ is $O(\Sigma_j'^2)$ and can be neglected when $W \ll 1$. Thus, we arrive at the following SDOS formula.

$$n_j^{\text{EM}}(\phi, E) = \frac{Z_j \Omega_j \Gamma_j / 4}{(E - E_j)^2 + (\Gamma_j / 2)^2}, \quad (49)$$

where

$$\Gamma_j = \hbar/\tau_j = -2Z_j\Sigma_j'' \quad (50)$$

is the inverse lifetime of the O-mode ($j = 1$) and E-mode ($j = 2$).

The SDOS for the edge modes as a function of E/Δ is shown in the lower panels of Fig. 3. The solid red and dashed blue lines, obtained using Eq. (43), represent $n_1^{\text{EM}}(\phi, E)$ and $n_2^{\text{EM}}(\phi, E)$, respectively. Since $\phi = \pi/2m$ is in the O-mode branch and $W = 0.1$ is sufficiently small, the subgap SDOS is dominated by $n_1^{\text{EM}}(\phi, E)$. The open red circles are plots of the approximate formula (49) for the O-mode, demonstrating that Eq. (49) successfully reproduces SDOS of the edge mode at small W .

In Fig. 4, the inverse lifetime Γ_1 at $\phi = \pi/2m$ and $E = E_1$ is plotted as a function of $W < 0.1$. The W dependence of Γ_1 is qualitatively different between the chiral p -wave and other chiral states. As W increases from zero, Γ_1 in the chiral p -wave state increases proportionally to W^2 , while those in the other chiral states increase linearly with W . Therefore, the inverse lifetime in the chiral p -wave state is kept relatively small. Similar W dependence of the inverse lifetime is observed for SDOS calculated with the self-consistent gap function (see Appendix B).

The W difference of the inverse lifetime can be understood as follows. The surface self-energy Σ_1 is proportional to S_2 . The imaginary part of S_2 of $O(W)$ is given by

$$S_2'' = 2W \langle \text{Im}[G_2^R] \rangle_\phi = 4W \langle n_2^{\text{EM}}(\phi, E) \rangle_\phi. \quad (51)$$

It follows that diffuse scattering between O- and E-modes is responsible for the linear increase of the inverse lifetime with W . The W^2 dependence of Γ_1 in the chiral p -wave state is because the edge mode has only a single branch. In this case, the finite inverse lifetime is caused by diffuse scattering via continuum states.

C. SDOS in the diffuse limit

Diffuse scattering causes the mixing of O- and E-modes. In the case of $W \ll 1$, the mode mixing is weak that subgap SDOS of the edge mode is described by $n_1(\phi, E)$ or $n_2(\phi, E)$. However, when $W \simeq 1$, the classification of the edge mode into O- and E-modes is not useful because of significant mode mixing. In particular, when $W = 1$, we have $n_1(\phi, E) = n_2(\phi, E)$, as can be shown from the property $\hat{\gamma}^2 = -1$ ($S_1 S_2 = -1$) of $\hat{\gamma}$ at $W = 1$ [25, 26].

Figure 5(a) shows $n(\phi, E) = n_1(\phi, E) + n_2(\phi, E)$ for $m = \text{odd}$ (spin triplet) in the diffuse limit. The SDOS in the p -wave state has a peak structure within the bulk gap, while those in non- p -wave triplet states coincide with the normal-state value, $n(\phi, E) = 1$. To understand the origin of the difference between the p - and non- p -wave triplet states, we assume that $S_1 = S_2 = i$. This

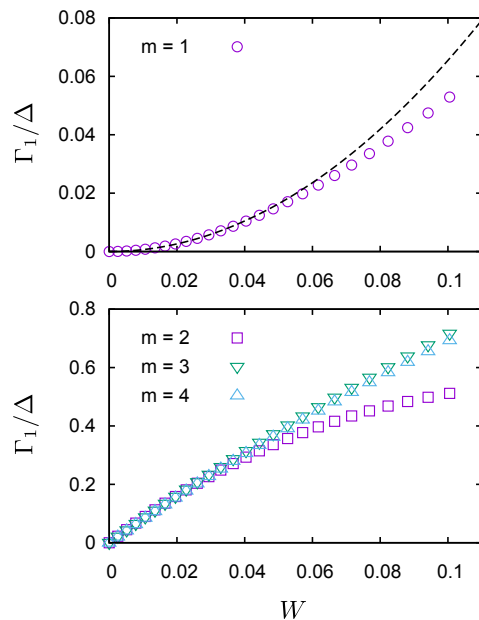


FIG. 4. Inverse lifetime Γ_1 at $\phi = \pi/2m$ and $E = E_1$ as a function of W . The dashed line in the upper panel shows W^2 dependence of the low W data.

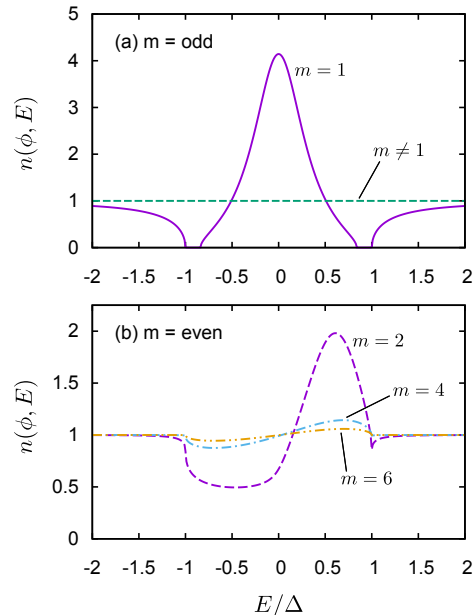


FIG. 5. Angle-resolved SDOS $n(\phi, E)$ at $\phi = \pi/2m$ in the diffuse limit for (a) $m = \text{odd}$ and (b) $m = \text{even}$. In the case of $m = \text{odd}$, $n(\phi, E) = 1$ except when $m = 1$.

assumption leads to $\mathcal{G}_1 = \mathcal{G}_2 = i$ [see Eqs. (35) and (36)]; hence, $n(\phi, E) = 1$. Substituting $S_1 = S_2 = i$ into the right-hand side of Eqs. (29) and (30), we obtain

$$S_1 = i(1 - \langle D(0) \rangle_\phi), \quad (52)$$

$$S_2 = i(1 + \langle D(0) \rangle_\phi). \quad (53)$$

It follows that the above assumption for $S_{1,2}$ is justified

if $\langle D(0) \rangle_\phi = 0$. Within the uniform gap model, we have

$$(m = 1) \quad \langle D(0) \rangle_\phi = \frac{\pi}{4i} \frac{\Delta}{\varepsilon + i\Omega}, \quad (54)$$

$$(m \neq 1) \quad \langle D(0) \rangle_\phi = \frac{1 + (-1)^m}{2(1 - m^2)} \frac{\Delta}{\varepsilon + i\Omega}. \quad (55)$$

Thus, $S_1 = S_2 = i$ is the self-consistent solution of $S_{1,2}$ for non- p -wave triplet states in the diffuse limit. This observation indicates that destructive interference due to diffuse scattering and anisotropic gap of chiral states results in $n(\phi, E) = 1$.

In Fig. 5(b), we show SDOS for $m = \text{even}$ (spin singlet) in the diffuse limit. In the singlet states, SDOS does not coincide with $n(\phi, E) = 1$ because of incomplete destructive interference. However, $n(\phi, E)$ approaches $n(\phi, E) = 1$ as m increases, as implied by Eq. (55), which shows that the destructive interference becomes increasingly complete as m increases.

The results confirm that SDOS in the diffuse limit is almost structureless except for the chiral p - and d -wave superconductors. This conclusion is not altered even when considering the spatial variation of the self-consistent gap function (see Appendix B).

VI. CONCLUSION

We studied the rough surface effect on the edge mode in 2D chiral superconductors to elucidate how robust the edge mode is to diffuse surface scattering. Specifically, we analyze the lifetime of the edge mode extracted from the angle-resolved SDOS formulated using the random S-matrix theory. We showed that when there are multiple branches of the edge mode, inter-branch scattering occurs due to diffuse scattering, considerably shortening the lifetime of the edge mode. Multiple branches arise in the higher order (non- p -wave) chiral superconductors. In contrast, in the chiral p -wave state, only a single branch exists, resulting in a robust edge mode.

In addition, we investigated the rough surface effect in the diffuse limit, where lifetime analysis is less meaningful due to strong branch mixing. The diffuse limit behavior of SDOS is understood qualitatively in terms of destructive interference, such as in unconventional superconductors with impurities. The destructive interference renders SDOS almost structureless in the chiral states other than the chiral p - and d -wave states. In particular, SDOS in the spin-triplet non- p -wave chiral state coincides with that in the normal state. The results confirm the findings of Suzuki and Asano [20] for the edge current density.

Our theory is sufficiently general to cover edge modes other than those in chiral superconductors, such as include flat-band edge modes, which have received considerable attention in the context of non-chiral d -wave superconductivity in cuprates [28–35]. As in the chiral case, the wave function for the flat band can be classified into

two groups, and the inter-branch scattering broadens the flat band. In fact, the flat-band broadening is significant in d -wave superconductors [34, 35] but not in p -wave superconductors [18, 24]. It should be noted, however, that unlike the chiral case the SDOS broadening for the flat band is accompanied by a peculiar V-shaped structure at $E = 0$ [34]. The origin of this structure remains an open question for future investigation.

ACKNOWLEDGMENTS

This work was supported in part by the JSPS KAKENHI Grant No. 22K03530.

Appendix A: Quasiclassical Green's function

The quasiclassical Green's function can be constructed in terms of two-component amplitude obeying the Andreev equation (7) with E replaced by the complex energy ε . The Andreev equation has damping (φ_α^d) and growing (φ_α^g) solutions with asymptotic behaviors

$$\varphi_+^d(y \rightarrow \infty) \propto \hat{\rho}_1 \varphi_-^d(y \rightarrow \infty) \propto \left(\frac{1}{D(\infty)} \right) e^{-\kappa y}, \quad (A1)$$

$$\varphi_+^g(y \rightarrow \infty) \propto \hat{\rho}_1 \varphi_-^g(y \rightarrow \infty) \propto \left(\frac{F(\infty)}{1} \right) e^{\kappa y}, \quad (A2)$$

where

$$D(\infty) = \frac{\Delta e^{-im\phi}}{\varepsilon + i\Omega}, \quad F(\infty) = \frac{\Delta e^{im\phi}}{\varepsilon + i\Omega}, \quad \kappa = \frac{\Omega}{\hbar v_\perp}, \quad (A3)$$

and $\hat{\rho}_1$ is the first Pauli matrix in the particle-hole space. We introduce new amplitudes

$$|y, l\alpha\rangle = \hat{\rho}_3 \varphi_\alpha^l(y), \quad \langle y, l\alpha| = [\hat{\rho}_1 \varphi_\alpha^l(y)]^T, \quad (A4)$$

where $l = d, g$ and the superscript T denotes transpose. These amplitudes obey

$$\alpha i \hbar v_\perp \partial_y |y, l\alpha\rangle = -\hat{h}_\alpha(y, \phi, \varepsilon) |y, l\alpha\rangle, \quad (A5)$$

$$\alpha i \hbar v_\perp \partial_y \langle y, l\alpha| = \langle y, l\alpha| \hat{h}_\alpha(y, \phi, \varepsilon). \quad (A6)$$

It follows readily from Eqs. (A5) and (A6) that the Wronskian

$$[\varphi_\alpha^g(y)]^T (-i \hat{\rho}_2) \varphi_\alpha^d(y) = \langle y, g\alpha | y, d\alpha \rangle = -\langle y, d\alpha | y, g\alpha \rangle$$

is a non-zero constant, and $|y, l\alpha\rangle \langle y, l'\alpha|$ satisfies the Eilenberger equation (Eq. (12)). From the observation, we arrive at the following expressions for $\hat{g}_\pm(y)$ that reproduce the bulk form given in Eq. (14).

$$\hat{g}_+(y) = \frac{2i}{\langle y, g+ | y, d+ \rangle} |y, d+ \rangle \langle y, g+ | - i, \quad (A7)$$

$$\hat{g}_-(y) = \frac{2i}{\langle y, d- | y, g- \rangle} |y, g- \rangle \langle y, d- | - i. \quad (A8)$$

Using Eqs. (A7) and (A8), we convert the surface boundary condition (17) to that for the Andreev amplitudes. The result can be written in the form

$$|0, g-\rangle \propto \frac{1 - i\hat{\gamma}}{1 + i\hat{\gamma}} |0, d+\rangle, \quad (\text{A9})$$

$$\{0, d-\} \propto \{0, g+\} \frac{1 + i\hat{\gamma}}{1 - i\hat{\gamma}}. \quad (\text{A10})$$

In the specular limit, these are reduced to

$$\varphi_-^g(0) \propto \varphi_+^d(0), \quad (\text{A11})$$

$$\varphi_+^g(0) \propto \varphi_-^d(0). \quad (\text{A12})$$

Equations (A11) and (A12) have a simple physical meaning. For $E > \Delta$ ($\varepsilon = E + i0^+$), the growing and damping solutions at $y = \infty$ correspond to incoming and outgoing waves, respectively. Thus, in Eq. (A11), the general growing solution $\varphi_-^g(y)$ (with a damping component mixed) represents such a scattering process that an incoming electron-like quasiparticle is Andreev reflected as a hole-like one. The simultaneously occurring normal reflection is described by $\varphi_+^d(y)$ that represents an outgoing electron-like quasiparticle. The amplitudes of the normal and Andreev reflections at a specular surface are determined from Eq. (A11). Equation (A12) determines these reflection amplitudes for a hole-like wave incoming toward the surface. Equations (A9) and (A10) are a generalization of Eqs. (A11) and (A12) to the rough surface case, respectively.

It is useful to note that the Andreev amplitude has the particle-hole symmetry $\varphi_+^l(y) \propto \hat{\rho}_1 \varphi_-^l(y)$. Thus, we introduce the parameterization

$$\varphi_+^d(y) = u_+^d(y) \begin{pmatrix} 1 \\ D(y) \end{pmatrix} \propto \hat{\rho}_1 \varphi_-^d(y), \quad (\text{A13})$$

$$\varphi_-^g(y) = u_-^g(y) \begin{pmatrix} 1 \\ F(y) \end{pmatrix} \propto \hat{\rho}_1 \varphi_+^g(y). \quad (\text{A14})$$

Substituting these into Eqs. (A7) and (A8) yields

$$\hat{g}_+(y) = \frac{2i\hat{\rho}_3}{1 - D(y)F(y)} \begin{pmatrix} 1 \\ D(y) \end{pmatrix} (1 - F(y)) - i. \quad (\text{A15})$$

$$\hat{g}_-(y) = \frac{2i\hat{\rho}_3}{1 - D(y)F(y)} \begin{pmatrix} 1 \\ F(y) \end{pmatrix} (1 - D(y)) - i. \quad (\text{A16})$$

From Eq. (A9), we obtain

$$\begin{pmatrix} 1 \\ F(0) \end{pmatrix} \propto \hat{\rho}_3 \frac{1 - i\hat{\gamma}}{1 + i\hat{\gamma}} \hat{\rho}_3 \begin{pmatrix} 1 \\ D(0) \end{pmatrix}. \quad (\text{A17})$$

Equation (A10) leads to the same result as Eq. (A17) because of particle-hole symmetry.

Functions $D(y)$ and $F(y)$ obey the Riccati-type differential equations

$$i\hbar v_\perp \partial_y D = 2\varepsilon D - \Delta_+^*(y, \phi) - \Delta_+(y, \phi) D^2, \quad (\text{A18})$$

$$i\hbar v_\perp \partial_y F = -2\varepsilon F + \Delta_-^*(y, \phi) + \Delta_-(y, \phi) F^2. \quad (\text{A19})$$

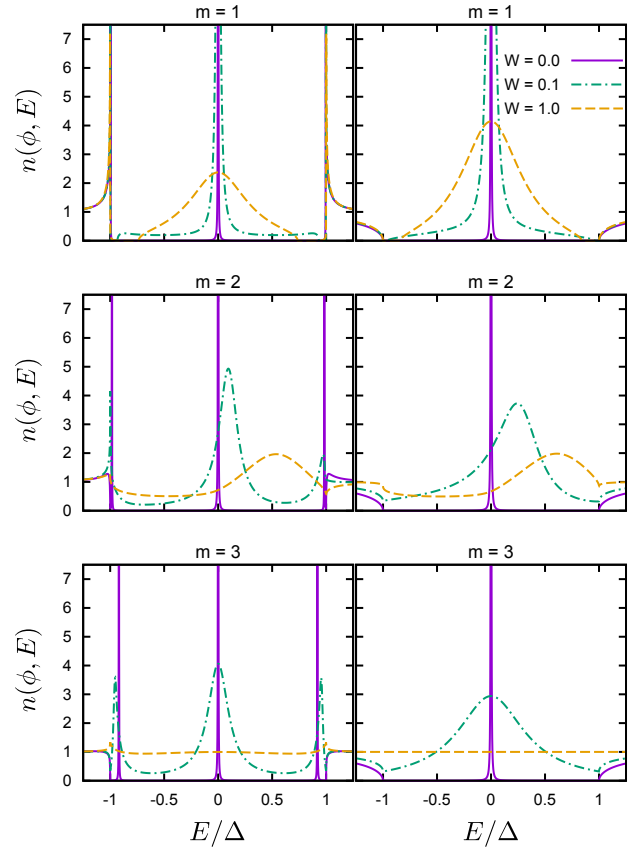


FIG. 6. Angle-resolved SDOS at $\phi = \pi/2m$ for $m = 1, 2, 3$ and $W = 0.0, 0.1, 1.0$. The left panels are the results computed with the self-consistent gap function. The right panels are those under the uniform gap model.

The functions $D(y)$ and $F(y)$ can be obtained as follows: First, we integrate Eq. (A18) from $y = \infty$ with the initial value $D(\infty)$ given in Eq. (A3). Next, we substitute the obtained $D(0)$ into Eq. (A17) to find $F(0)$. Finally, Eq. (A19) is integrated from $y = 0$.

Appendix B: SDOS under the self-consistent gap function: Comparison to the uniform gap model

The numerical results of SDOS presented in the main text are obtained under the uniform gap model. Here, we discuss the influence of the spatially varying self-consistent gap function on SDOS.

The left (right) panels of Fig. 6 show the angle-resolved SDOS at $\phi = \pi/2m$ computed with the self-consistent (uniform) gap function. When the surface is specular (solid violet lines), the self-consistent SDOS has sharp peaks corresponding to edge modes of two: the gapless mode, which is the focus of this paper, and high-energy modes with $|E|$ close to the bulk gap edge [14]. The peaks of the high-energy modes are absent in SDOS under the uniform gap model. This is because the high-energy modes appear due to the suppression of $\Delta^a(y, \phi)$

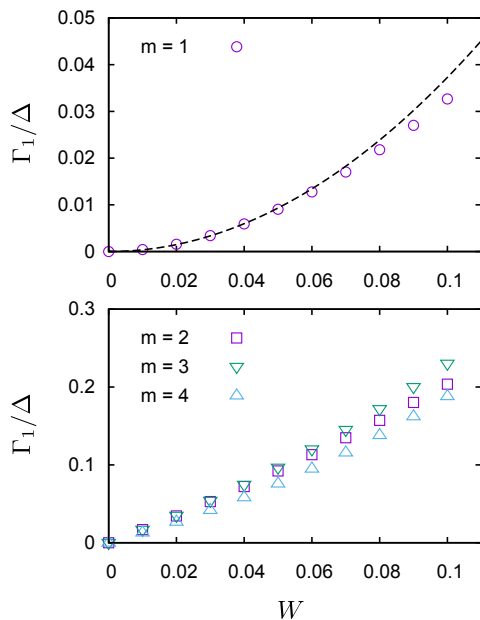


FIG. 7. Inverse lifetime Γ_1 as a function of W for the same parameters of ϕ and E as those in Fig. 4. The results are computed with the self-consistent gap function.

at the surface (see Fig. 1) and are bound states trapped by the potential valley formed between the surface and suppressed $\Delta^a(y, \phi)$ [14].

Note that quasiparticles specularly scattered at the surface undergo a difference in sign of $\Delta^a(y, \phi)$ between the incoming and outgoing trajectories. Such scattering processes are known to suppress $\Delta^a(y, \phi)$ at the surface [24]. In the chiral p -wave state, quasiparticles can experience the sign change of $\Delta^a(y, \phi)$ in any scattering channel. Thus, $\Delta^a(y, \phi)$ is strongly suppressed in the specular and diffuse limits. In contrast, in the higher-order chiral states, there are scattering channels in which $\Delta^a(y, \phi)$ maintains its sign, weakening the suppression when the surface is rough. Therefore, the uniform gap model fairly agrees with the self-consistent SDOS for $W = 0$ (dashed yellow lines) in the higher-order chiral states.

Except for the high-energy modes, the uniform gap model captures the qualitative features of the self-consistent SDOS. In particular, the inverse lifetime extracted from the self-consistent SDOS by Lorentzian fitting reproduces the W dependence predicted by the uniform gap model, i.e., a linear and quadratic increase from $W = 0$ in the chiral p -wave state and other chiral states, respectively (Figs. 4 and 7).

-
- [1] D. Vollhardt and P. Wölfle, *The Superfluid Phases of Helium 3* (Taylor & Francis, 1990).
- [2] Y. Maeno, H. Hashimoto, K. Yoshida, S. Nishizaki, T. Fujita, J. G. Bednorz, and F. Lichtenberg, Superconductivity in a layered perovskite without copper, *Nature* **372**, 532 (1994).
- [3] T. M. Rice and M. Sigrist, Sr_2RuO_4 : an electronic analogue of ^3He ?, *J. Phys.: Condens. Matter* **7**, L643 (1995).
- [4] Y. Maeno, S. Kittaka, T. Nomura, S. Yonezawa, and K. Ishida, Evaluation of spin-triplet superconductivity in Sr_2RuO_4 , *J. Phys. Soc. Jpn.* **81**, 011009 (2012).
- [5] Y. Maeno, S. Yonezawa, and A. Ramires, Still mystery after all these years —unconventional superconductivity of Sr_2RuO_4 —, *J. Phys. Soc. Jpn.* **93**, 062001 (2024).
- [6] M. Matsumoto and M. Sigrist, Quasiparticle states near the surface and the domain wall in a $p_x \pm ip_y$ -wave superconductor, *J. Phys. Soc. Jpn.* **68**, 994 (1999).
- [7] M. Stone and R. Roy, Edge modes, edge currents, and gauge invariance in $p_x + ip_y$ superfluids and superconductors, *Phys. Rev. B* **69**, 184511 (2004).
- [8] J. A. Sauls, Surface states, edge currents, and the angular momentum of chiral p -wave superfluids, *Phys. Rev. B* **84**, 214509 (2011).
- [9] Y. Tsutsumi and K. Machida, Edge mass current and the role of Majorana fermions in A -phase superfluid ^3He , *Phys. Rev. B* **85**, 100506(R) (2012).
- [10] T. Mizushima, Y. Tsutsumi, T. Kawakami, M. Sato, M. Ichioka, and K. Machida, Symmetry-protected topological superfluids and superconductors —from the basics to ^3He —, *J. Phys. Soc. Jpn.* **85**, 022001 (2016).
- [11] W. Huang, E. Taylor, and C. Kallin, Vanishing edge currents in non- p -wave topological chiral superconductors, *Phys. Rev. B* **90**, 224519 (2014).
- [12] Y. Tada, W. Nie, and M. Oshikawa, Orbital angular momentum and spectral flow in two-dimensional chiral superfluids, *Phys. Rev. Lett.* **114**, 195301 (2015).
- [13] X. Wang, Z. Wang, and C. Kallin, Spontaneous edge current in higher chirality superconductors, *Phys. Rev. B* **98**, 094501 (2018).
- [14] E. Sugiyama and S. Higashitani, Surface bound states and spontaneous edge currents in chiral superconductors: Effect of spatially varying order parameter, *J. Phys. Soc. Jpn.* **89**, 034706 (2020).
- [15] P. Holmval and A. M. Black-Schaffer, Enhanced chiral edge currents and orbital magnetic moment in chiral d -wave superconductors from mesoscopic finite-size effects, *Phys. Rev. B* **108**, 174505 (2023).
- [16] P. E. C. Ashby and C. Kallin, Suppression of spontaneous supercurrents in a chiral p -wave superconductor, *Phys. Rev. B* **79**, 224509 (2009).
- [17] Y. Nagato, S. Higashitani, and K. Nagai, Subgap in the edge states of two-dimensional chiral superconductor with rough surface, *J. Phys. Soc. Jpn.* **80**, 113706 (2011).
- [18] S. V. Bakurskiy, A. A. Golubov, M. Y. Kupriyanov, K. Yada, and Y. Tanaka, Anomalous surface states at interfaces in p -wave superconductors, *Phys. Rev. B* **90**, 064513 (2014).
- [19] S. Lederer, W. Huang, E. Taylor, S. Raghu, and C. Kallin, Suppression of spontaneous currents in Sr_2RuO_4 by surface disorder, *Phys. Rev. B* **90**, 134521 (2014).
- [20] S.-I. Suzuki and Y. Asano, Spontaneous edge current in a small chiral superconductor with a rough surface, *Phys. Rev. B* **94**, 155302 (2016).
- [21] S. V. Bakurskiy, N. V. Klenov, I. I. Soloviev, M. Y.

- Kupriyanov, and A. A. Golubov, Observability of surface currents in p -wave superconductors, *Supercond. Sci. Technol.* **30**, 044005 (2017).
- [22] S.-I. Suzuki and A. A. Golubov, Robustness of chiral surface current and subdominant s -wave Cooper pairs, *Phys. Rev. B* **108**, 134501 (2023).
- [23] Y. Nagato, S. Higashitani, K. Yamada, and K. Nagai, Theory of rough surface effects on the anisotropic BCS states, *J. Low Temp. Phys.* **103**, 1 (1996).
- [24] Y. Nagato, M. Yamamoto, and K. Nagai, Rough surface effects on the p -wave fermi superfluids, *J. Low Temp. Phys.* **110**, 1135 (1998).
- [25] K. Nagai, Y. Nagato, M. Yamamoto, and S. Higashitani, Surface bound states in superfluid ^3He , *J. Phys. Soc. Jpn.* **77**, 111003 (2008).
- [26] N. Miyawaki and S. Higashitani, Influence of diffuse surface scattering on the stability of superconducting phases with spontaneous surface current generated by Andreev bound states, *Phys. Rev. B* **98**, 134516 (2018).
- [27] G. Eilenberger, Transformation of Gorkov's equation for type II superconductors into transport-like equations, *Z. Phys.* **214**, 195 (1968).
- [28] C.-R. Hu, Midgap surface states as a novel signature for $d_{x_a^2-x_b^2}$ -wave superconductivity, *Phys. Rev. Lett.* **72**, 1526 (1994).
- [29] Y. Tanaka and S. Kashiwaya, Theory of tunneling spectroscopy of d -wave superconductors, *Phys. Rev. Lett.* **74**, 3451 (1995).
- [30] Y. Nagato and K. Nagai, Surface and size effect of a d_{xy} -state superconductor, *Phys. Rev. B* **51**, 16254 (1995).
- [31] S. Higashitani, Mechanism of paramagnetic Meissner effect in high-temperature superconductors, *J. Phys. Soc. Jpn.* **66**, 2556 (1997).
- [32] M. Håkansson, T. Löfwander, and M. Fogelström, Spontaneously broken time-reversal symmetry in high-temperature superconductors, *Nat. Phys.* **11**, 755 (2015).
- [33] P. Holmvall, A. B. Vorontsov, M. Fogelström, and T. Löfwander, Broken translational symmetry at edges of high-temperature superconductors, *Nat. Commun.* **9**, 2190 (2018).
- [34] M. Matsumoto and H. Shiba, On boundary effect in d -wave superconductors, *J. Phys. Soc. Jpn.* **64**, 1703 (1995).
- [35] K. Yamada, Y. Nagato, S. Higashitani, and K. Nagai, Rough surface effects on d -wave superconductors, *J. Phys. Soc. Jpn.* **65**, 1540 (1996).